

## Supplementary Figure Legends

### Figure S1. PARP1 regulates PARP2 recruitment and retention in human RPE-1 cells

(A) The targeting scheme of *Parp1* conditional mice and southern blot of successfully targeted ES clones. The schematic diagram represents the murine *Parp1* locus (top), targeting vector (2nd row), targeted allele (3rd row), and the neo-deleted allele (*Parp1*<sup>C</sup>, bottom). The southern probe is marked as thick black lines and the exons and FRT sequences are shown as black solid boxes and open triangles, respectively. Restriction site designation: Scal. The map is not drawn to scale. (B) Western blot of endogenous *Parp1* and *Parp2* proteins in WT, *Parp1* KO, *Parp2* KO, and *Parp1/2* DKO iMEF cells. (C) The kinetics of mRFP-XRCC1 foci (relative intensity) in *Parp2* KO and *Parp1/2* DKO iMEF cells in the presence and absence of niraparib. (D) The normalized PARP2 intensity at DNA damage sites in *Parp2* KO and *Parp1/2* DKO iMEFs in the presence and absence of niraparib. (E) Western blot of endogenous PARP1 and PARP2 levels in wild type, *PARP1* KO, *PARP2* KO, and *PARP1/2* DKO RPE-1 cells. (F) Representative images of GFP-PARP2 and mRFP-XRCC1, and (G) the relative intensity kinetics of GFP-PARP2 at DNA damage sites in *PARP2* KO and *PARP1/2* DKO RPE-1 cells in the presence and absence of niraparib. (H) The maximal relative intensity of GFP-PARP2. The dots and bars represent means and SEM, respectively, from one representative experiment out of 2–4 with  $n > 8$  cells each time with consistent results. The two-tailed unpaired Student's t-test. ns,  $p > 0.05$ ; \*\* $p < 0.01$ ; \*\*\* $p < 0.001$ .

### Figure S2. The time of photobleaching does not affect recovery kinetics and niraparib also enhances PARP2 foci from 8-MOP primed cells.

(A) The relative intensity of GFP-PARP2 before photobleaching at 3 min post-irradiation in *PARP1/2* DKO RPE-1 cells in the presence and absence of PARP inhibitors. (B) Calculated FRAP recovery curves for GFP-PARP2 foci photo-bleached at the 60s and 180s post-irradiation in *PARP1/2* DKO RPE-1 cells without PARP inhibitors.  $t_{1/2} = 1.3 \pm 0.9s$ ,  $B_{max} = 88.7 \pm 3.3\%$  for 60s;  $t_{1/2} = 1.6 \pm 0.7s$ ,  $B_{max} = 90.3 \pm 2.5\%$  for 180s.  $P$ -value was calculated based on the extra sum-of-square  $F$  test. ns,  $p > 0.05$ . (C) Representative images of GFP-PARP2 and mRFP-XRCC1 upon 60% 405 nm laser-induced micro-irradiation in *PARP1/2* DKO RPE-1 cells in the presence and absence of 8-MOP. (D) Representative images of GFP-PARP2 and mRFP-XRCC1, and the relative intensity kinetics of (E) GFP-PARP2 and (F) mRFP-XRCC1 upon 20% 405nm laser-induced micro-irradiation in 8-MOP treated *PARP1/2* DKO RPE-1 cells in the presence and absence of niraparib. (G) The relative intensity of GFP-PARP2 before photobleaching at 3 min post-irradiation in 8-MOP treated *PARP1/2* DKO RPE-1 cells in the presence and absence of niraparib. (H and J) The maximal relative intensity of (H) GFP-PARP2, and (J) mRFP-XRCC1 in *PARP1* KO RPE-1 cells in the presence and absence of niraparib. (I) The relative intensity of GFP-PARP2 before photobleaching at 3 min post-irradiation in *PARP1* KO RPE-1 cells in the presence and absence of niraparib. The dots and bars represent means and SEM, respectively, from one representative experiment out of 2–4 with  $n > 8$  cells each time with consistent results. The two-tailed unpaired Student's t-test. \*\*\* $p < 0.001$ .

### Figure S3 Trapping of PARP2 required the physical presence of niraparib in MEF cells.

(A) CD spectrometry measurement of purified WT and EA/HA mutant PARP2 (0.2 mg/mL) in 20 mM Potassium Phosphate (pH 7.5), 0.1 mM EDTA, 0.1 mM TCEP. All spectra are reported in Mean Residue Ellipticity. (B-D) Representative pNick release data for (B) human PARP2 WT, (C) murine *Parp2*-H404A, and (D) *Parp2*-E534A with NAD<sup>+</sup>. (E) Representative pNick release data for WT and mutant PARP2 in the presence of purified HPF1. (F) Binding affinity of WT-PARP2 and H404A-Parp2 to the pNick model DNA substrate. The calculated  $K_d$  were marked under the graph.

### Figure S4 PARP2 trapping in niraparib treated iMEF cells does not correlate with PARP2 activity.

(A) Representative images of GFP-PARP2 WT, E545A, H415A, and mRFP-XRCC1 in *Parp1/2* DKO iMEFs. (B) the relative intensity kinetics of PARP2 WT, E545A, and H415A at DNA damage sites in *PARP1/2* DKO RPE-1 cells in the presence and absence of niraparib. (C and D) The maximal relative

intensity of (C) GFP-PARP2 WT, E545A and H415A, and (D) mRFP-XRCC1. (E) The relative intensity of GFP-PARP2-E545A and -H415A before photo-bleaching at 3 min post-irradiation in *PARP1/2* DKO RPE-1 cells in the presence and absence of niraparib. The dots and bars represent means and SEM, respectively, from one representative experiment out of 2–4 with  $n > 8$  cells each time with consistent results. The two-tailed unpaired Student's t-test. ns,  $p > 0.05$ ; \* $p < 0.05$ ; \*\* $p < 0.01$ ; \*\*\* $p < 0.001$

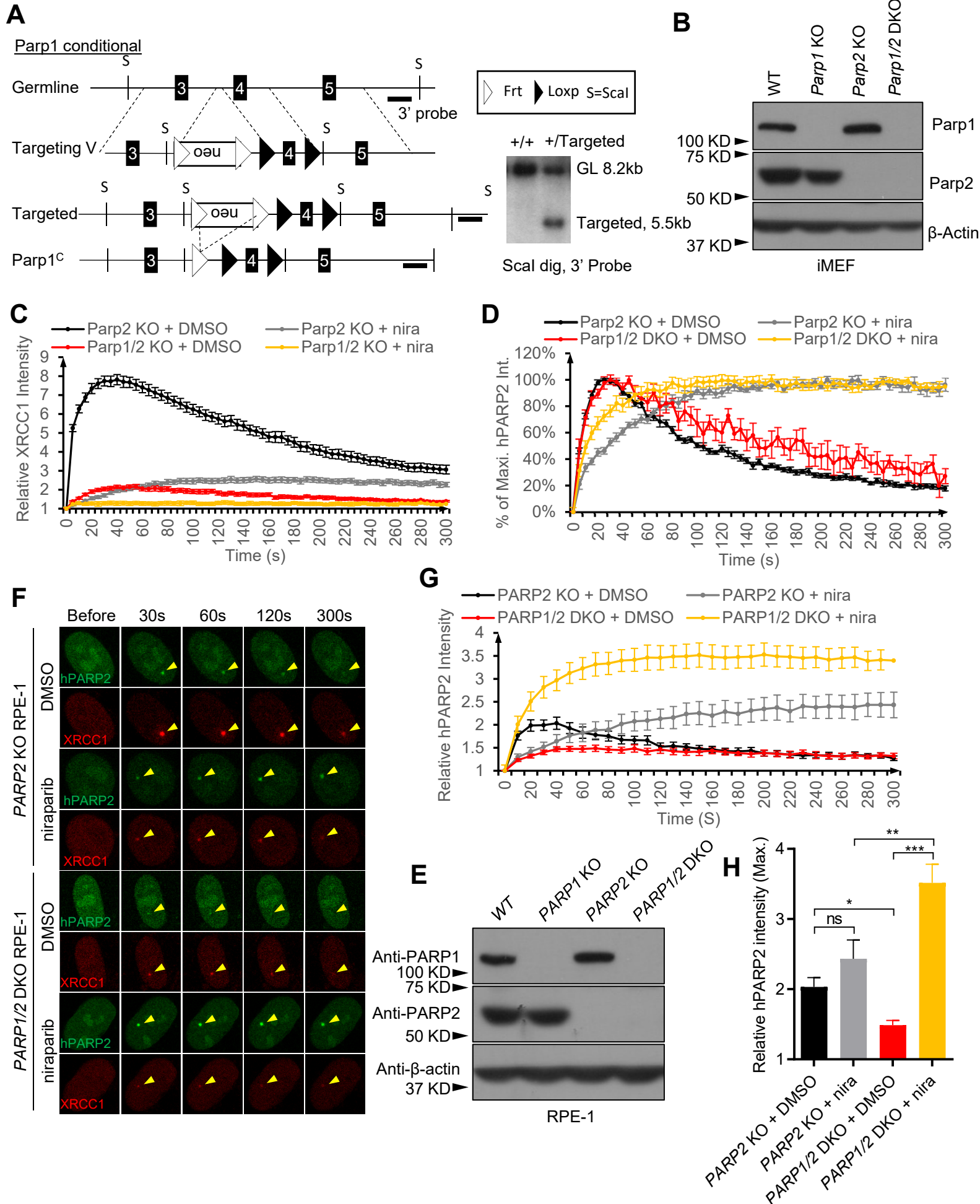
**Figure S5 NTR does not affect PARP2 foci formation.**

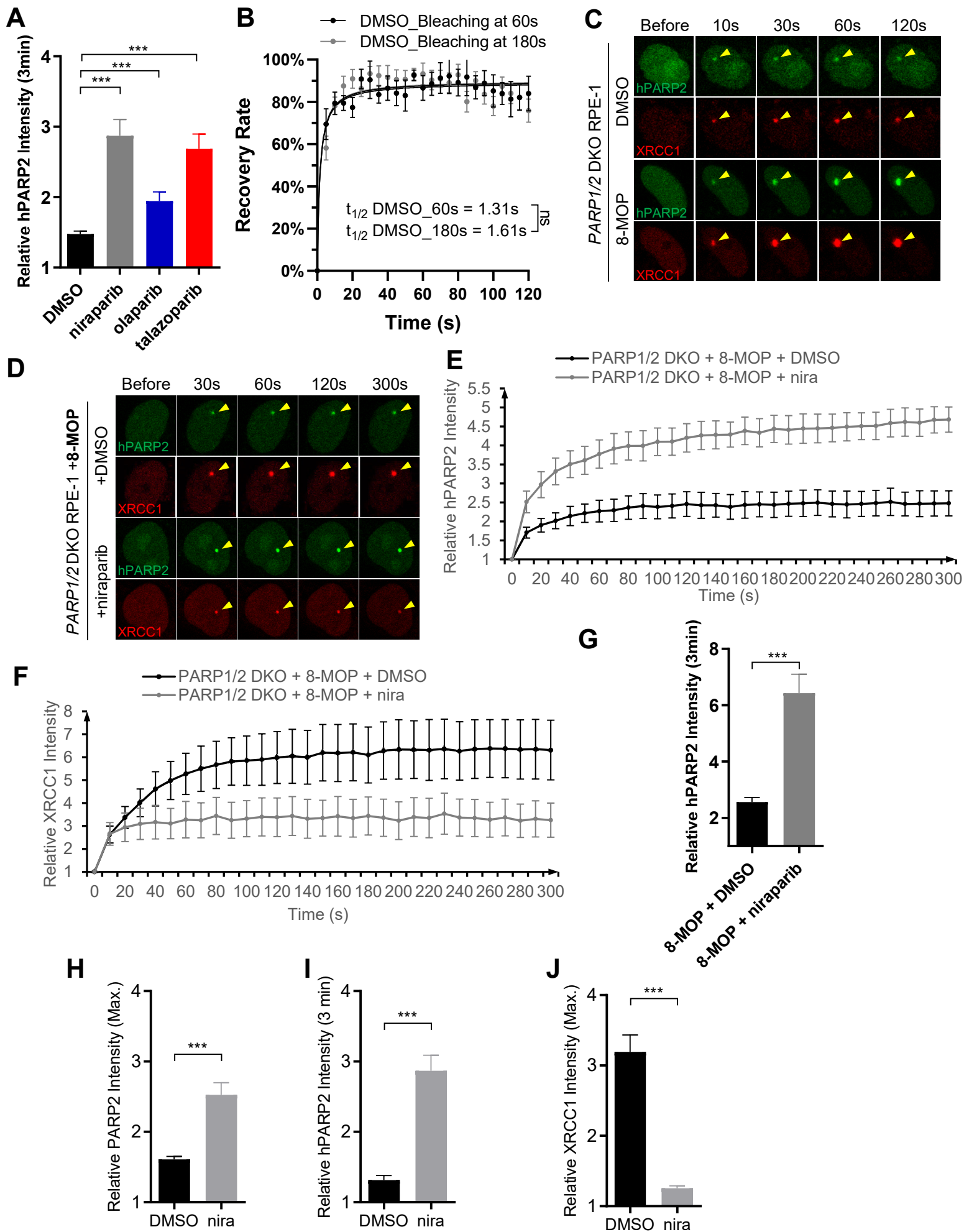
(A) Representative images of GFP-PARP2 WT, PARP2<sup>ΔNTR</sup> (Δ1-70aa), PARP2<sup>88-570</sup>, and mRFP-XRCC1 in *PARP1/2* DKO cells. (B) The relative intensity kinetics of GFP-PARP2 WT, PARP2<sup>ΔNTR</sup>, and PARP2<sup>88-570</sup> at DNA damage sites in *PARP2* KO and *PARP1/2* DKO RPE-1 cells. (C and D) The maximal relative intensity of (C) GFP-PARP2 WT, PARP2<sup>ΔNTR</sup> and PARP2<sup>88-570</sup>, and (D) mRFP-XRCC1. (E) Alignment of the N-terminal region of human (isoform 1 and 2) and mouse PARP2 from the Uniprot database. The aa in red are those that differ in the small and large NTR deletion.

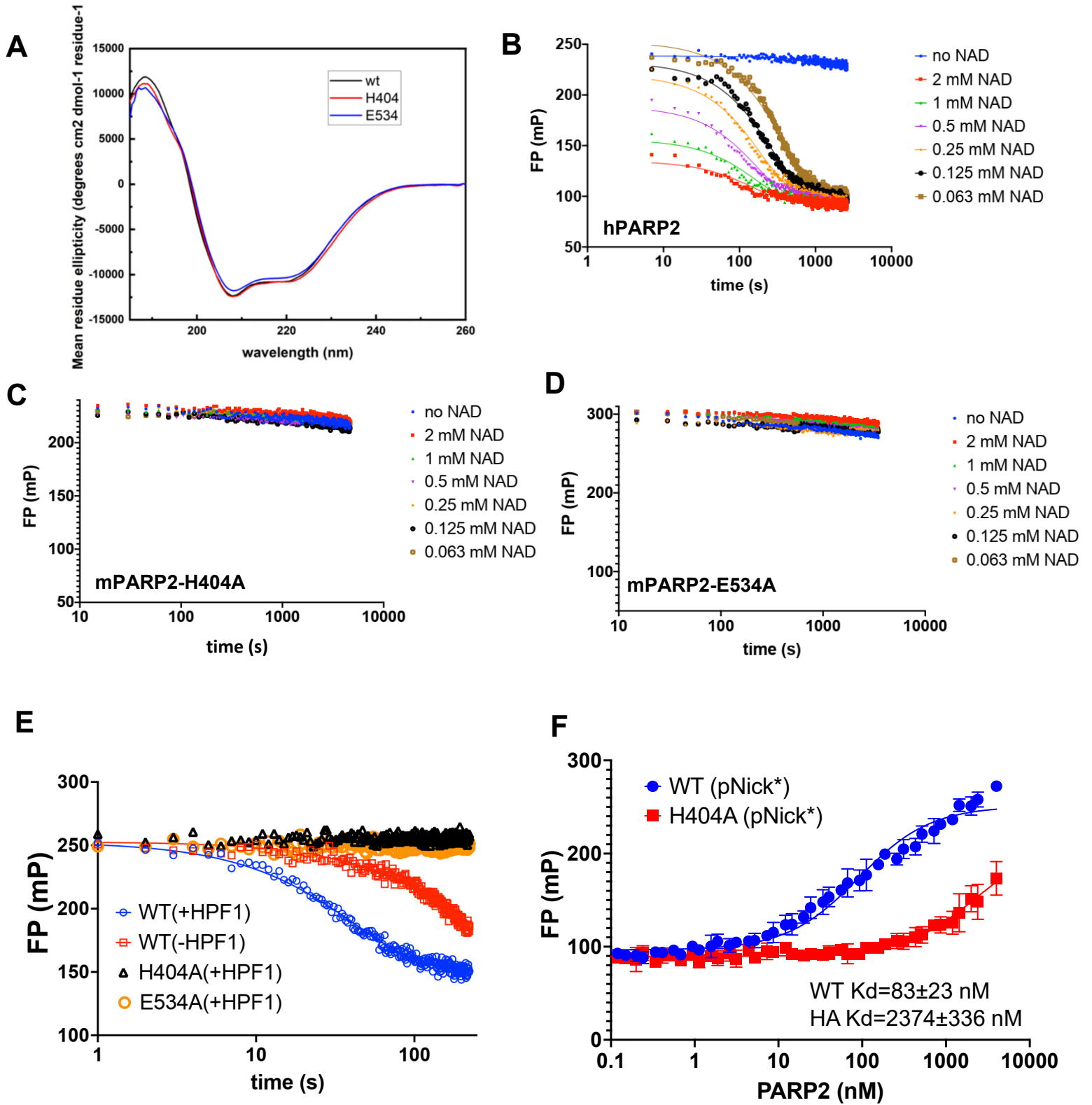
**Figure S6 Niraparib abolished PARP2 R140A foci, but not PARP2 WT foci in PARP1 proficient RPE-1 cells.**

(A) Representative images of GFP-PARP2 WT, R140A, and mRFP-XRCC1 in PARP1 proficient RPE1 cells. (B) The relative intensity kinetics of GFP-PARP2 WT and R140A at DNA damage sites in *PARP2* KO (PARP1-proficient) RPE-1 cells in the presence and absence of niraparib. (C and D) The maximal relative intensity of (C) GFP-PARP2 WT and R140A, and (D) mRFP-XRCC1. The dots and bars represent means and SEM, respectively, from one representative experiment out of 2–4 with  $n > 8$  cells each time with consistent results. The two-tailed unpaired Student's t-test. ns,  $p > 0.05$ ; \* $p < 0.05$ ; \*\* $p < 0.01$ ; \*\*\* $p < 0.001$ . (E) Soluble and chromatin fraction of *PARP1* KO RPE-1 cells and *PARP1/2* DKO RPE-1 cells ectopically expressing PARP2-R140A that are treated with MMS (0.1 mg/mL, 1 hr) and/or niraparib (1 μM, 1 hr). (F) Flow cytometry analyses of the frequency of hCD8 positive *PARP1/2* DKO + empty-hCD8 and *PARP1/2* DKO + hCD8/PARP2<sup>RA</sup> RPE-1 cells at day 0 and day 6 of niraparib sensitivity assay. (G) Niraparib sensitivity assay for WT, *PARP1* KO, *PARP1/2* DKO + hCD8 and *PARP1/2* DKO + hCD8/PARP2<sup>RA</sup>. The dots and error bars represent means and SEM, respectively, from one representative experiment out of 3 consistent biological repeats with triplicate samples per experiment. *P* value of IC50 was calculated using the extra sum-of-square *F* test. ns,  $p > 0.05$ ; \*\*\* $p < 0.001$ .

# Figure S1



**Figure S2**

**Figure S3**

**Figure S4**

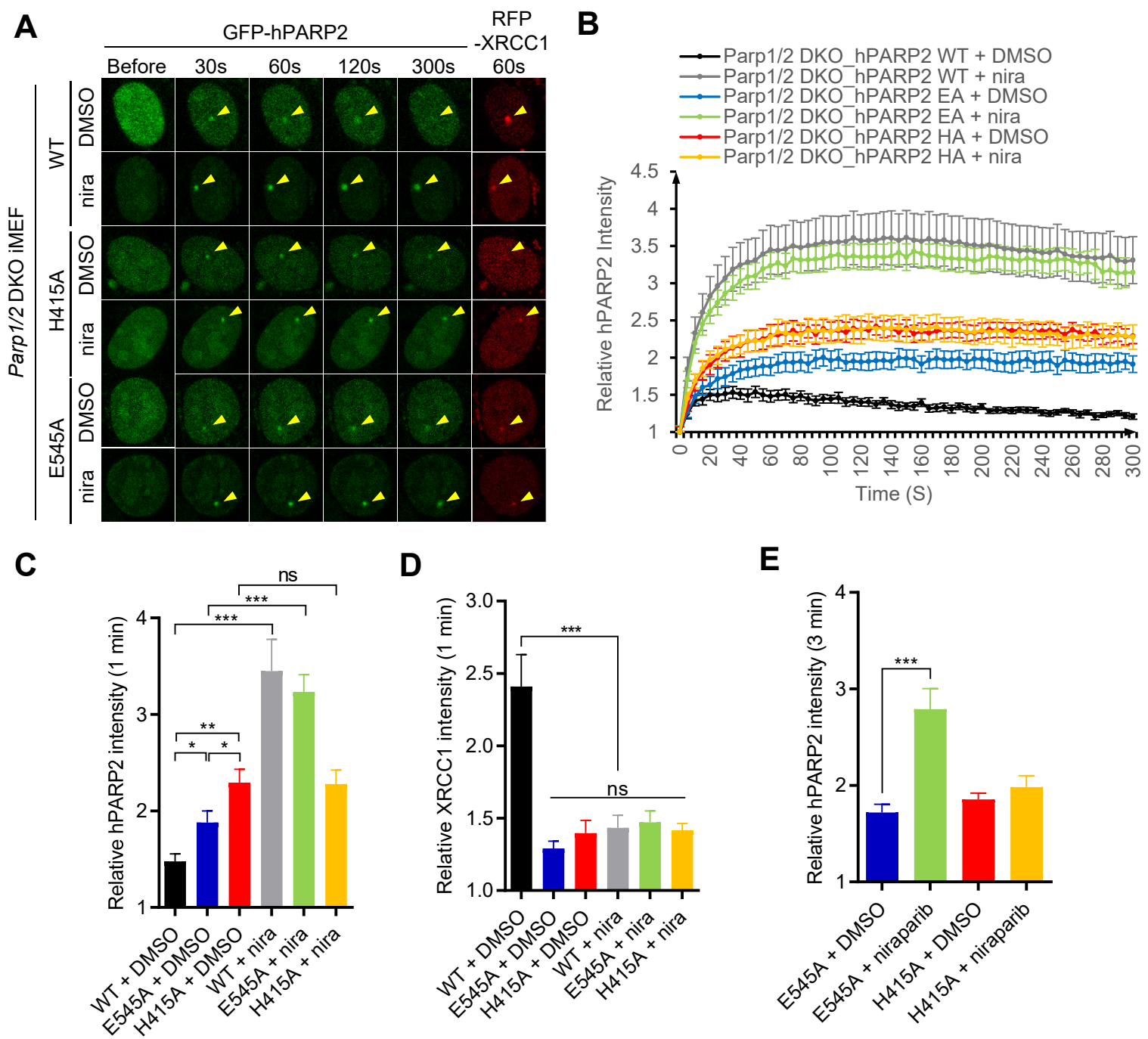
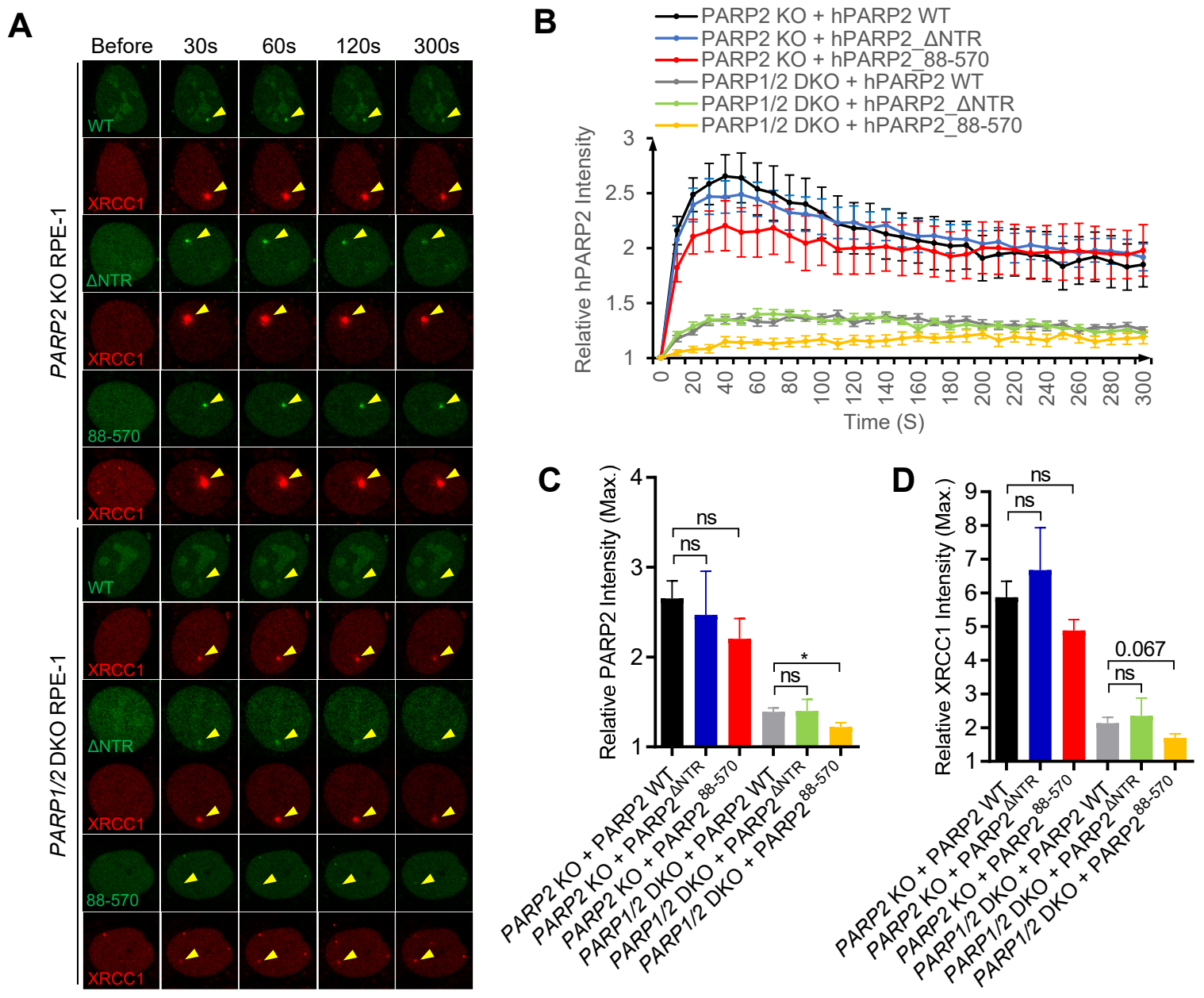




**Figure S5**



**E**

hPARP2 (iso.1) MAARRRRSTGGGRARALNESKRVNNGNTAPEDSSP-AKKTRRCQRQESKKMPVAGGKANK 59  
hPARP2 (iso.2) MAARRRRSTGGGRARALNESKRVNNGNTAPEDSSP-AKKTRRCQRQESKKMPVAGGKANK 59  
mPARP2 MAPRRQR--SGSGRRVLNEAKKVDNGNKATEDDSSPPGKKMRTCQRK----GPMAGGKDAD 54  
\*\* \*\*: \* . \* . \* . \* \* \* : \* \* : \* \* \* . \* \* \* . \* \* \* \* \* : \* : \* \* \* \*

hPARP2 (iso.1) DRTEDKQDGMPPGRSWASKRVSESVKALLLK GKAPVDPECTAKVGVKAHVYCEGNDVYDVML 119  
hPARP2 (iso.2) DRTEDKQD-----ESVKALLLK GKAPVDPECTAKVGVKAHVYCEGNDVYDVML 106  
mPARP2 -RT-----KDNRDSVKTLLLK GKAPVDPECAAKLGVKAHVYCEGDDVYDVML 99  
\*\* : \* \* \* : \* \* \* \* \* \* \* \* \* \* : \* \* : \* \* \* \* \* \* \* \* : \* \* \* \* \* \*

aa 71-87 different in long vs short NTR deletion

**Figure S6**

